International Journal of Thermophysics, Vol. 24, No. 2, March 2003 (© 2003)

Effect of Air Oxidation on the Thermophysical Properties of a Zirconium Alloy[1]

I. I. Petrova,[2,3] V. E. Peletsky,[2] B. N. Samsonov,[2] A. V. Nikulina,[4] N. B. Sokolov,[4] and L. N. Andreeva-Andrievskaya[4]

The results of an experimental study of the effect of air oxidation on the temperature dependence of the heat capacity and normal spectral emissivity (for the wavelength of 0.65 μm) of the zirconium alloy E635 (~ 1.3 mass% Sn, ~ 0.3 mass% Fe, ~ 1 mass% Nb) are presented. The subsecond resistive pulse heating technique has been used. The samples were heated in ambient air by single and multiple cyclic pulses.

KEY WORDS: heat capacity; spectral emissivity; subsecond resistive pulse heating; zirconium alloy.

1. INTRODUCTION

Zirconium-based alloys are used in nuclear reactors for the envelopes of fuel elements and other components. For the safety analysis of nuclear reactors, the accident situation must be examined when the temperature of fuel elements is dramatically increased up to the melting point. Accurate data on the thermophysical properties of zirconium alloys at high temperatures for the prediction of the behavior of nuclear fuel elements is therefore necessary.

In a previous paper [1], we described the use of a subsecond pulse heating technique for the study of the thermophysical properties of a

[1] Paper presented at the Fourteenth Symposium on Thermophysical Properties, June 25–30, 2000, Boulder, Colorado, U.S.A.

[2] Institute for High Energy Densities, Associated Institute for High Temperatures, Izhorskaya 13/19, 125412 Moscow, Russia.

[3] To whom correspondence should be addressed. E-mail: iipetrova@rambler.ru

[4] Federal State Unitary Enterprise, VNIINM, Rogova 5a, 123060 Moscow, Russia.

0195-928X/03/0300-0533/0

Zr-0.01Nb-0.003Fe-0.013Sn alloy in an inert (argon) atmosphere. In the present work the experiments have been carried out in conditions similar to possible accidents—rapid heating and an oxidizing ambient atmosphere. The oxidizing atmosphere makes noticeable effects on the properties of the zirconium alloy at high temperatures and especially in the temperature range of the α–β phase transition. The samples used in these experiments were made from commercial tubes of nuclear fuel element envelopes.

2. EXPERIMENTAL MEASUREMENTS

The technique of subsecond pulse resistive heating [2] of samples with a high density of direct current ($\sim 5000\ \mathrm{A \cdot cm^{-2}}$) from room temperature up to the melting temperature with a heating rate of about $1000\ \mathrm{K \cdot s^{-1}}$ was used. The length of the tubular samples was ~ 75 mm; their external diameter was ~ 9.1 mm and their internal diameter was ~ 7.7 mm. The nominal distance between two probes in the central part of the sample, where the voltage drop was measured, was 10 mm. The blackbody model for measurement of the true temperature was made with a rectangular slit, 20 mm long and 1 mm wide in the wall of the tubular sample. The effective emissivity for such a blackbody was found experimentally and was equal to 0.89 [3]. The model with these parameters ensures an isothermal field along the working section [4] during heating at the rate mentioned above. Two high-speed photoelectric pyrometers (both with a wavelength of 0.65 μm) measured temperatures of the sample synchronously. One of them measured the brightness temperature of the surface (the lower limit of measurements was about 1600 K), the other one—the true temperature inside the blackbody (the lower limit was about 900 K). All the quantities (the electrical current I, the voltage drop along the central section U, the true temperature T_{tr}, and the brightness temperature T_{br}) were measured using an A/D-converter with a sample rate from 100 up to 1000 samples/s.

The heat capacity C_p and the spectral emissivity ε_λ (for a wavelength $\lambda = 0.65$ μm) were calculated with the following expressions:

$$C_p = \frac{UI - q_r}{m\left(\frac{dT}{d\tau}\right)_h} \tag{1}$$

$$\ln \varepsilon_\lambda = \frac{c_2}{\lambda}\left(\frac{1}{T_{\mathrm{tr}}} - \frac{1}{T_{\mathrm{br}}}\right) \tag{2}$$

In these expressions m is the mass of the central working section of the sample, $C_2 = 1.4388 \times 10^{-2}\ \mathrm{m \cdot K}$ is the second constant in Planck's law, $(dT/d\tau)_h$ is the heating rate, q_r is a correction for the radiation heat losses, and λ is the wavelength of the pyrometers.

3. EXPERIMENTAL RESULTS

3.1. Heating and Cooling Thermograms

Experiments were performed for four samples. The three samples were heated by a single pulse to different maximum temperatures: 1700, 1900, and 2100 K. The fourth sample was heated by multiple cyclic pulses (five times) to a maximum temperature of 1900 K and cooled to room temperature after each pulse. The increase of mass due to oxidation was measured after each experiment.

Figure 1 shows the dependence of $T_{tr} = f(\tau)$ (curve 1) and of $T_{br} = f(\tau)$ (curve 2) which have been measured in the experiment with single pulse heating up to 1900K in an air atmosphere. The heating stage of this experiment is shown in detail in Fig. 2. As we can see from Fig. 1, there is a peculiarity of these thermograms—abnormal behavior of temperature dependences on the cooling section. This is due to an exothermic oxidation reaction (with heat liberation). Intense oxidation takes place mainly during the cooling stage, as the process of the sample cooling is slower than for heating. Larger brightness temperatures over true ones at the cooling stage is caused by a difference of the heat liberation at oxidation of the external and internal surfaces of the tube sample. The conditions for oxidation near the external surface of the tube are better, as the transport of oxygen is

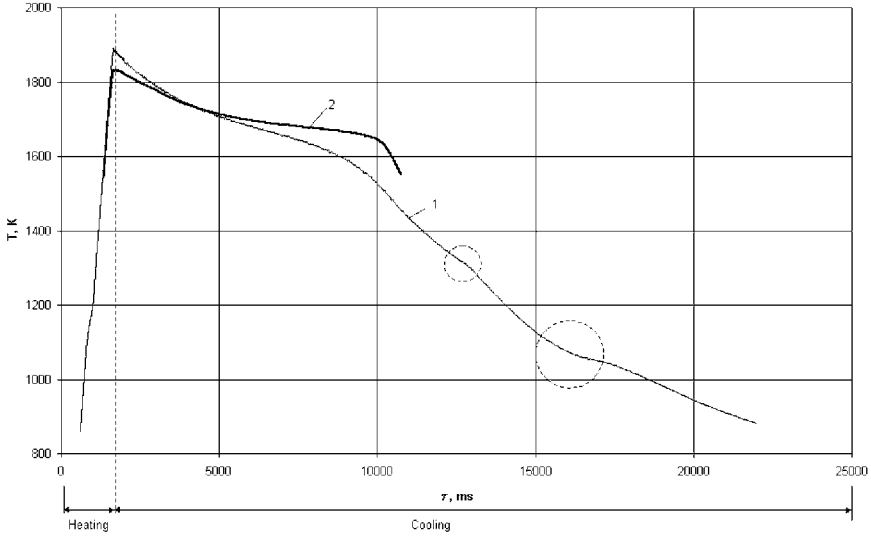

Fig. 1. True (1) and brightness (2) temperatures of the zirconium alloy for single pulse heating up to $T = 1900$ K.

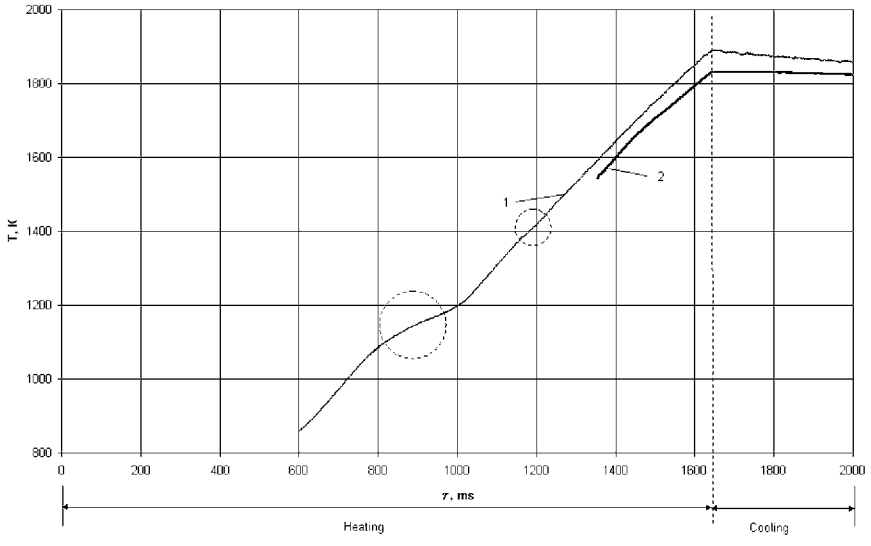

Fig. 2. Heating section of thermogram shown in Fig. 1 for the true (1) and brightness (2) temperatures.

larger in comparison to the internal surface, which is inside the closed volume. It is confirmed by the distribution of microhardness along the cross section of the tube samples after the experiments. The results of microhardness measurements are shown in Fig. 3. The first sample was heated by a single pulse to $T_{tr} = 1900$ K (curve 1), the second one—to $T_{tr} = 2100$ K (curve 2), and the third had five repeated cycles of pulse heating to $T_{tr} = 1900$ K (curve 3). The microhardness H_{50} distributions along the cross section of the tube is in accordance with the oxygen concentration. The microhardness in the central part of the tube wall is less than near the surfaces, and it is higher near the outer surface in comparison to the inner one. After five cycles of heating, there is an increase of microhardness in the central part of the tube wall. It means that the entire cross section of the tube was involved in oxygen dissolution.

After the single pulse heating and subsequent cooling in air a cross section of the sample consists of several components. There are an oxide film on the tube surfaces, deeper diffusion layers of the oxygen solid solution in the alloy with variable concentration along the cross section, and the pure alloy (without oxygen), which occupies the bigger part of the tube wall cross section. For a system like this, we can see two breaks (marked by the circles) on the thermograms (Figs. 1 and 2). The first break at $T_{tr} = 1100$ to 1200 K is the α–β transition in the alloy and in the adjoining diffusion layer. The small second break at $T_{tr} = 1300$ to 1400 K is the oxide film phase transition

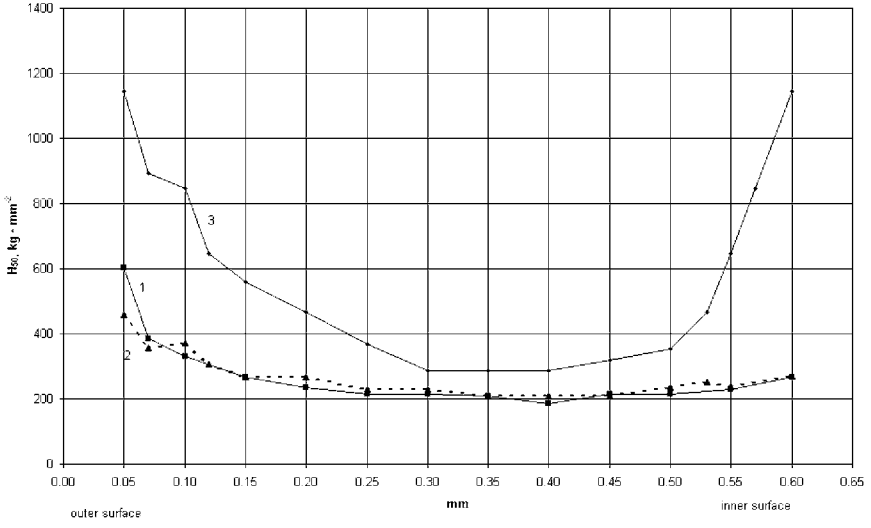

Fig. 3. Distribution of the microhardness H_{50} along the cross section of the tube wall after single pulse heating up to $T = 1900$ K (1); $T = 2100$ K (2); after repeated cycles of heating (5 pulses) up to $T = 1900$ K (3).

from a monoclinic to tetragonal lattice [4]. It is not very distinctly observed in the region of heating. As we can see from Figs. 1 and 2, the α–β phase transition temperature is higher in the heating stage in comparison to the cooling one. It can be explained by the delay in a new phase nucleation at high rate processes and by the significant difference between the heating and cooling rates.

Figure 4 shows the thermograms of the true (1) and the brightness (2) temperatures of the zirconium alloy sample heated by a single pulse in an air atmosphere up to $T_{tr} = 2100$ K. As we can see, the change of the cooling rate depends on the maximum temperature of heating. There is even a small temperature rise after switching off the electrical current, due to more intense oxidation in the initial stage of cooling in this higher temperature experiment.

Five heating-cooling cycles on the single sample in an air atmosphere were carried out, and the true temperature thermograms are shown in Fig. 5. For every cycle the sample was heated to $T_{tr} = 1900$ K and cooled to room temperature. The cooling stage of the first thermogram significantly differs from the following ones. As the initial sample surface was clear (not oxidized), a process of oxidation for the first heating-cooling cycle was more intense, and the heat liberation was higher than for the following ones. Therefore, the temperature on the cooling stage is higher, and the

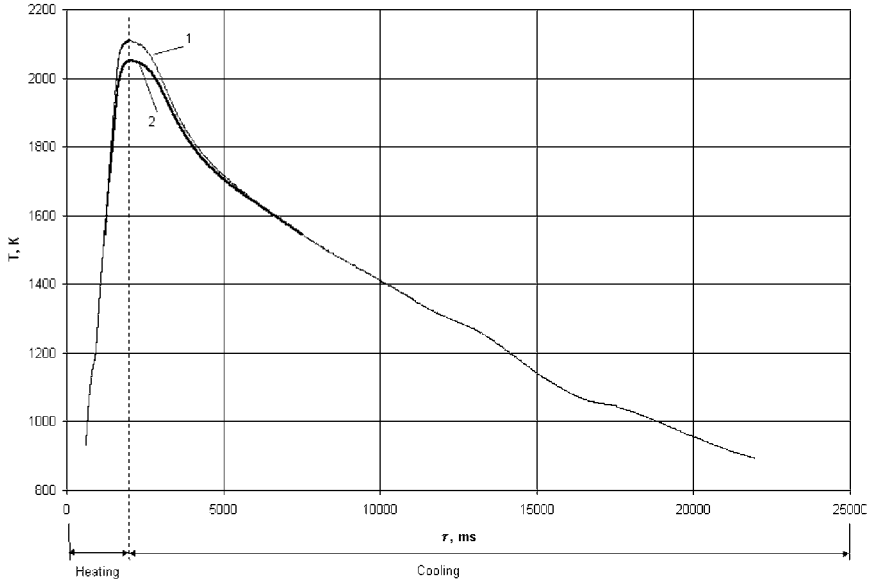

Fig. 4. True (1) and brightness (2) temperatures for single pulse heating up to $T = 2100$ K.

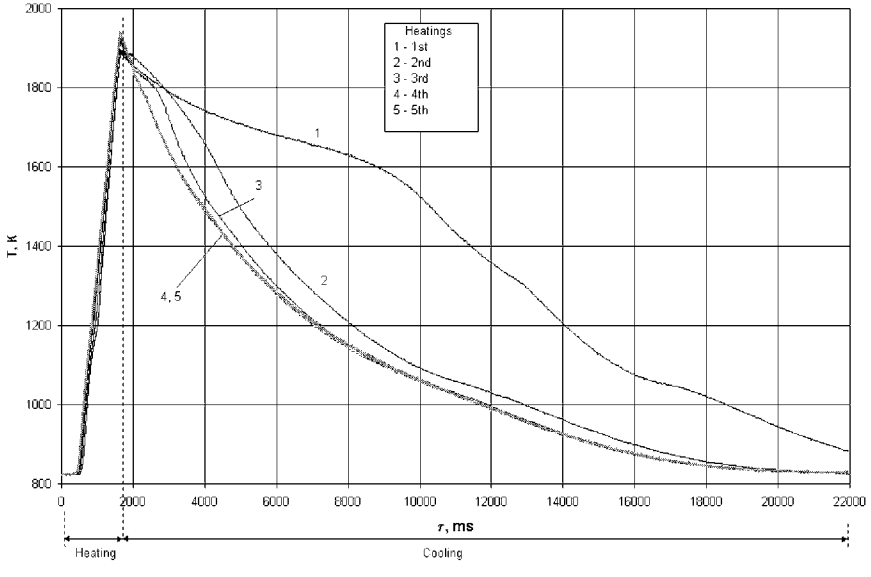

Fig. 5. True temperatures of the zirconium alloy for different numbers of pulse heating cycles on the single sample.

cooling rate is lower for the first cycle than for the following ones, as can be seen from Fig. 5.

After the first pulse heating, the sample surface was covered with dark (non-stoichiometric) oxide film, which was a barrier for oxidation for the following pulse heating. Therefore, the sample oxidation was less intense for the second pulse heating and following ones, as we can see from the cooling rates (Fig. 5, curves 2–5). After each cycle of heating-cooling, the color of the sample surface becomes lighter, i.e., the oxide film becomes more stoichiometric.

The α–β phase transition breaks on the thermograms (Fig. 5) become smoother with each successive pulse heating, i.e., the α–β phase transition temperature range grows due to an increase of oxygen concentration in the solid solution.

3.2. Heat Capacity

The temperature dependences of the heat capacity of zirconium alloy E635 for cyclic pulse heating (five cycles) in an air atmosphere are shown in Fig. 6. For the first pulse heating (curve 1), when the sample structure and composition represent practically the initial values, the first heat capacity peak is around $T_{tr} = 1170$ K, and it corresponds to the α–β phase transition of non-oxidized alloy. With every subsequent pulse heating, the oxygen concentration in the alloy increases. Therefore, the temperature range of

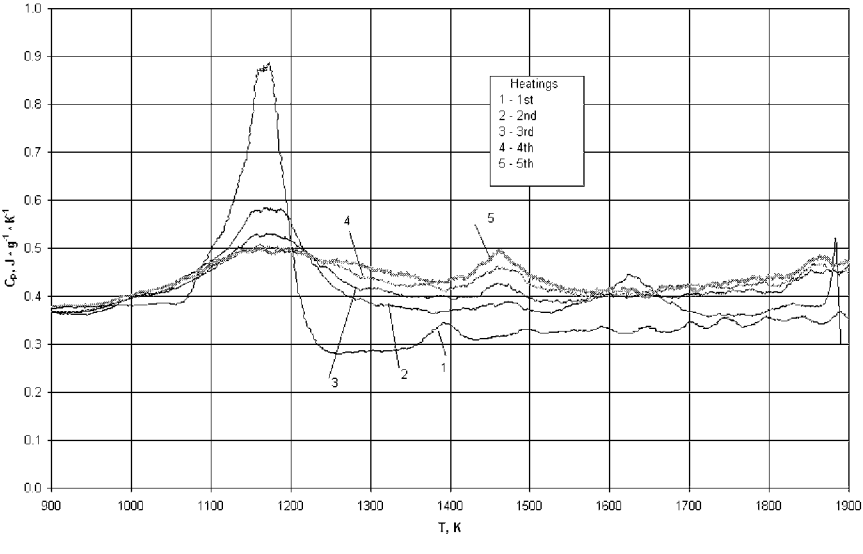

Fig. 6. Heat capacity for cyclic pulse heating of the sample in an air atmosphere.

the α–β phase transition expands, and the amplitude of the first peak decreases. The second small peak on curve 1 is near $T_{tr} = 1400$ K. It may be due to the heat consumption at dissolution of a thin oxide film, which is formed during the heating stage from oxygen, adsorbed by the sample surface.

A dark-colored non-stoichiometric oxide covers the sample after the first pulse heating. The larger quantity of the oxygen was absorbed at this stage (the increase of the sample mass after the first pulse heating was about three times greater than after the following ones). For the second heating and following ones, an oxygen-rich solid solution in near-surface layers is transformed to oxide, and the second peak at $T_{tr} = 1460$ K on the heat capacity curve represents the oxide structural transition from the monoclinic to the tetragonal modification. According to Ref. 5, the temperature of the equilibrium transition from a monoclinic to tetragonal structure is $T_{tr} = 1470$ K for stoichiometric zirconium oxide, and it is not far from our results. With every following heating cycle, the height of the second peak increases, and it is caused by the increase of the oxide film thickness.

The temperature dependences of the heat capacity of the same alloy in an argon atmosphere are shown in Fig. 7 for comparison. As can be seen from Figs. 6 and 7, there is a significant difference in the behavior of the heat capacity for heating in air and in argon.

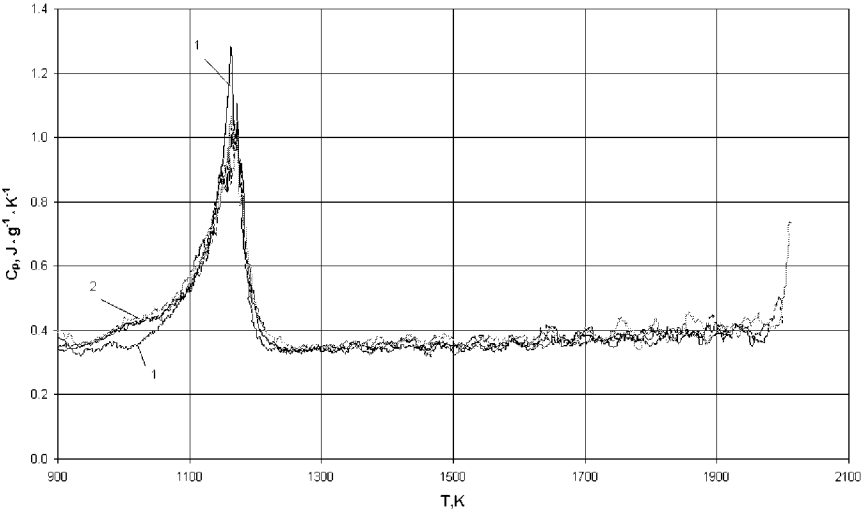

Fig. 7. Heat capacity for cyclic pulse heating of the sample in an argon atmosphere: (1) first heating; (2) all successive heatings.

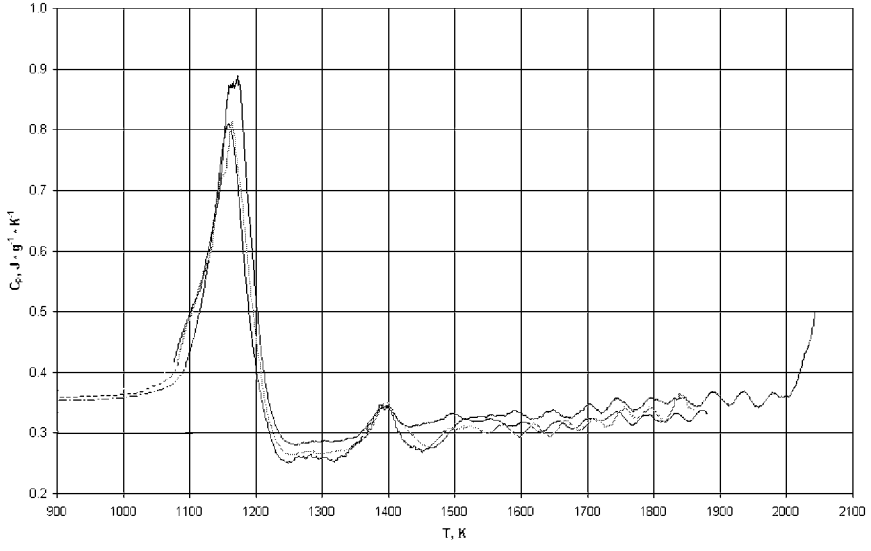

Fig. 8. Heat capacity of three various samples for the first heating.

The data on the heat capacity for the first heating in air for three different samples are shown in Fig. 8. The experimental data show good reproducibility for the phase-transition area.

3.3. Spectral Emissivity.

There is a significant difference between the absolute values and temperature dependence of the spectral emissivity $\varepsilon_\lambda = f(T)$ of the zirconium alloy E635 for heating in an air atmosphere and in argon. These results are shown in Fig. 9, where curves 1 and 2 are the results for two different samples for first heating in air, and curve 3 relates to an argon environment. Due to the presence of the oxide film on the sample surface for heating in air, the emissivity is significantly larger than for heating in argon. The temperature dependence $\varepsilon_\lambda = f(T_{\text{tr}})$ corresponds to the surface change during an oxidizing process. The increase of ε_λ at $T_{\text{tr}} > 2000$ K (Fig. 9, curve 2) may be associated with the increase of the outer wall temperature, due to the beginning of the intense oxidation and the heat liberation.

The temperature dependences of the spectral emissivity ε_λ of zirconium alloy E635 for cyclic pulse heating in air (five pulses) to $T_{\text{tr}} = 1900$ K are shown in Fig. 10. At the first pulse heating (curve 1), the emissivity ε_λ increases from ~ 0.6 to ~ 0.7 at $T_{\text{tr}} = 1600$ to 1700 K and then it decreases a little. The emissivity for the second pulse heating has abnormally high

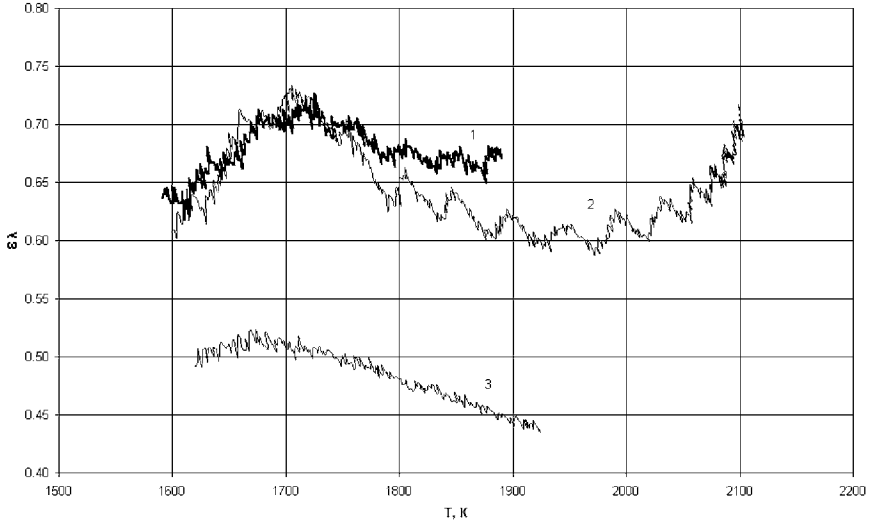

Fig. 9. Spectral emissivity for the first pulse heating in an air atmosphere (1), (2) and in argon (3).

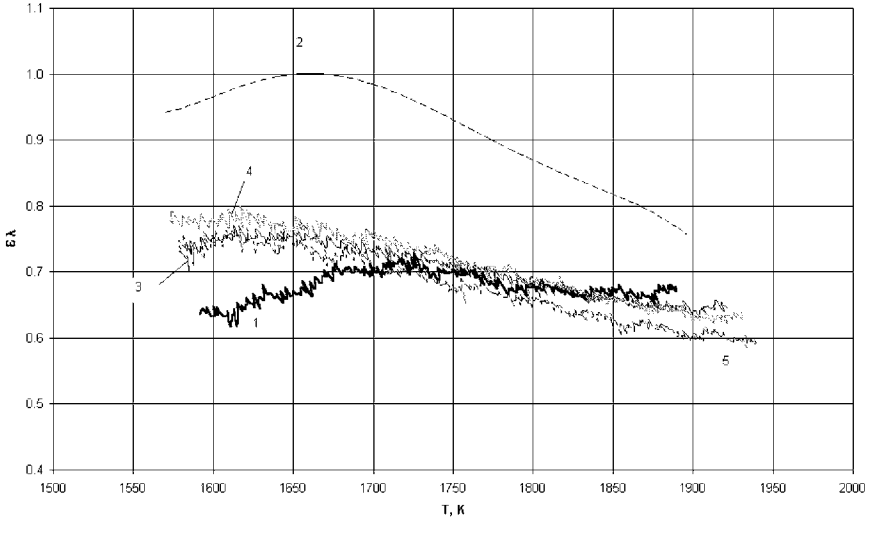

Fig. 10. Spectral emissivity for cyclic pulses of heating in air: (1) first heating; (2) second heating; (3) third heating; (4) fourth heating; (5) fifth heating.

values, because after the first pulse heating-cooling cycle, the sample surface became very dark and the emissivity was high. Additionally, the brightness temperature increases due to the larger heat liberation on the outer surface, as was discussed above. Thus we have incorrect results for emissivity for the second pulse heating, and we show it with a dotted line (curve 2, Fig. 10). For the third and fourth pulse heatings, the temperature dependences of emissivity are the same and decrease from ~ 0.75 to ~ 0.6 with an increase of temperature from $T_{\text{tr}} = 1600$ to 1900 K. For the fifth pulse heating, $\varepsilon_\lambda = f(T)$ is displaced a little lower.

4. CONCLUSION

A series of experiments have been carried out with the purpose of studying the influence of an oxidizing environment (ambient air atmosphere) on thermophysical properties of zirconium alloy E635. The subsecond technique has been used for resistive heating of zirconium alloy samples, which were made from the commercial envelopes of the fuel elements of nuclear reactors.

Significant differences in the results are observed for heating of the samples in an air atmosphere in comparison to an inert environment at the same other conditions of heating. The reasons involve both the formation of oxide film on a sample surface, and the oxygen diffusion into the samples. The appearance of the second peak on the heat capacity curve (in addition to the peak of the α–β phase transition in the alloy), which corresponded to the phase transition in oxide film, is the specific feature of heating in an air atmosphere. The position and the amplitude of the first and second peaks on the heat capacity curve are changed for every succeeding heating pulse, and they are correlated with sample oxidizing dynamics. The amplitude of the first peak on the curves $C_p = f(\tau)$ decreases, and the amplitude of the second peak increases, when the number of the pulses heating cycles increases. It is explained by increases in the oxygen concentration dissolved in the alloy, and increases in the oxide film thickness. Absolute values of C_p in the β-phase increase with every successive heating pulse, as the sample becomes more saturated with oxygen.

The change of the temperature dependences of the spectral emissivity for rapid heating in an air atmosphere correlates with the oxidizing dynamics of the sample. Formation of oxide film on the sample surface for the first pulse heating is accompanied by an increase of emissivity. For the second pulse there is abnormally high values of emissivity, due to influence of the additional heat liberation at the outer surface. The gradual transformation of a dark (non-stoichiometric) film to a white (stoichiometric)

film with every successive heating pulse leads to a small decrease of emissivity. The absolute values ε_λ for heating in an air atmosphere are larger than in an argon environment over the complete measured temperature range.

ACKNOWLEDGMENT

This work has been supported by the Russian Foundation for Basic Research (Project No. 99-02-18258).

REFERENCES

1. V. E. Peletsky, I. I. Petrova, B. N. Samsonov, A. V. Nikulina, N. B. Sokolov, and L. N. Andreeva-Andrievskaya, in *Proc. Conf. Thermophysical Aspects of WWER-Type Reactor Safety*, Vol. 2, A. D. Efanov, ed. (Ministry of Russian Federation for Atomic Energy, Institute of Physics and Power Engineering, Obninsk, 1998), p. 162.
2. I. I. Petrova and V. Ya. Chekhovskoi, *Teplofiz. Vys. Temp.* **26**:271 (1988).
3. I. I. Petrova and V. E. Peletsky, *High Temp.* **33**:710 (1995).
4. V. E. Peletsky, *High Temp.* **37**:123 (1999).
5. R. J. Ackermann, S. P. Garg, and E. G. Rauh, *J. Amer. Ceramic Society* **60**:341 (1977).